D. SŁOTA*

RECONSTRUCTION OF THE BOUNDARY CONDITION IN THE PROBLEM OF THE BINARY ALLOY SOLIDIFICATION

ODTWORZENIE WARUNKU BRZEGOWEGO W ZAGADNIENIU KRZEPNIĘCIA STOPU DWUSKŁADNIKOWEGO

The solution of the inverse problem involving the designation of the boundary condition in the problem of the binary alloy solidification for known temperature measurements at a selected point of the cast is presented. In the discussed model, the temperature distribution is described by means of the Stefan problem with varying in time temperature corresponding to the beginning of solidification and depending on the concentration of the alloy component. Whereas to describe the concentration, the Scheil model was used.

Keywords: : solidification, inverse problems, binary alloy, macrosegregation

W pracy przedstawiono rozwiązanie zagadnienia odwrotnego polegającego na określeniu warunku brzegowego w zagadnieniu krzepnięcia stopu dwuskładnikowego, gdy znane są pomiary temperatury w wybranym punkcie odlewu. W rozważanym modelu rozkład temperatury opisany został zagadnieniem Stefana ze zmienną w czasie temperaturą odpowiadającą początkowi procesu krzepnięcia, zależną od stężenia składnika stopowego. Do opisu stężenia wykorzystano model Scheila.

1. Introduction

The inverse problem provides a very useful tool for analyses of various processes [8, 9, 17, 28, 30]. Inverse problems are used, when the causes of the described phenomenon are unknown or not completely defined. An explicit solution of such problem requires additional information, for example, the temperature measurements at given points of the domain.

The Stefan problem poses an important case of heat transfer processes, involving mathematical models describing heat processes characterized by the phase changes. For example: metal solidification, crystal growth, food freezing, ice melting, etc. The Stefan problem consists in the simultaneous designation of the temperature distribution in the investigated domain and the location of the phase change boundary, separating the given domain to the sub-domains occupied by the liquid and solid phases. In the inverse Stefan problem it is usually assumed that the additional information, compensating the absence of the input data, is partial knowledge of the location of the phase change boundary, its velocity towards the normal direction or the temperature at selected points of the domain. The direct and inverse Stefan problems are nonlinear problems. Their non-linearity is the consequence of the Stefan condition [18].

The inverse Stefan problem was discussed in numerous works [6, 19, 22, 26, 34, 35]. For example, in papers [6, 22, 26] application of the Adomian decomposition method, the variation iteration method and the homotopy perturbation method to the approximate solution of one-phase inverse Stefan problem were discussed. Whereas, in [5,23-25] numerical algorithms enabling the approximate solution of the multi-dimensional and multi-phase inverse Stefan problem were presented.

The issues of macrosegregation and the solidification of binary alloy were considered in [10, 12-14, 16, 20, 21, 27, 29, 31, 32]. The majority of available publications are focused on direct problems. The inverse problem is discussed in [3, 4, 21, 33].

In the model analyzed in the current paper the temperature distribution is described by the Stefan problem [2, 7, 15], where the solidification temperature depends on the concentration of the alloy component. To describe the concentration of the alloy component the Scheil model was used [1, 14]. This model is derived by assuming the limiting form of the real course of the macrosegregation process. In the solidifying material the diffu-

* SILESIAN UNIVERSITY OF TECHNOLOGY, INSTITUTE OF MATHEMATICS, 44-100 GLIWICE, 23 KASZUBSKA STR., POLAND

sion occurs both in the liquid phase, as well as in the solid one. Because of diffusion coefficient in the solid phase (D_2) is considerably smaller than the one in the liquid phase (D_1), it is assumed in the Scheil's model that $D_2 = 0$, whereas, $D_1 \rightarrow \infty$. The discussed problem entails the designation of the heat transfer coefficient on the boundary of the domain, where temperature measurements are known for the selected point of the cast.
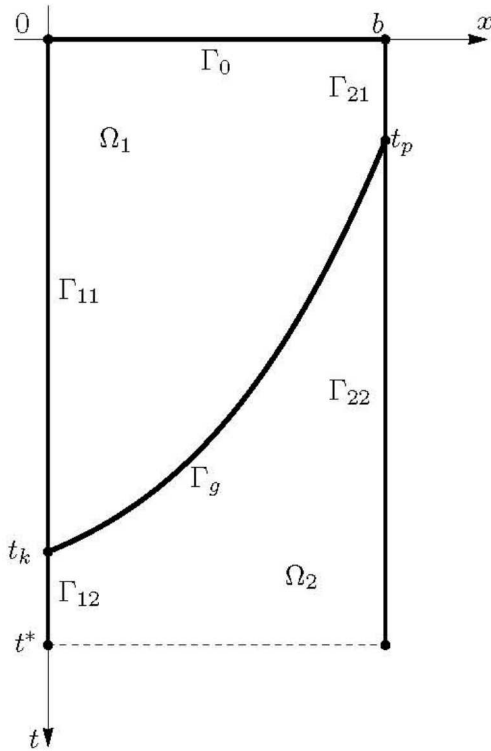

Fig. 1. Domain of the problem

2. Formulation of the problem

In domain Ω, occupied by a solidifying material, two sub-domains changing with time are considered: Ω_1 occupied by the liquid phase and Ω_2 occupied by the solid phase (Fig. 1). These domains are separated by the phase change boundary Γ_g (moving boundary), which is determined by varying in time liquidus temperature (or the, so called, equivalent solidification point [14]). Temperature distribution in each of the phases is determined by the following heat conduction equation (i =1,2):

$$c_i \varrho_i \frac{\partial T_i}{\partial t}(x,t) = \lambda_i \frac{\partial^2 T_i}{\partial x^2}(x,t), \qquad (1)$$

for $x \in \Omega_i, t \in (0, t^*)$, where c_i, ϱ_i and λ_i are the specific heat, the mass density and the thermal conductivity in the liquid phase ($i = 1$) and solid phase ($i = 2$), and t

and x refer to time and spatial location, respectively. On the boundary Γ_0 the following initial condition is given ($T_0 > T^*(Z_0)$):

$$T_1(x, 0) = T_0, \qquad (2)$$

where T_0 is the initial temperature, T^* is the temperature of solidification, Z_0 is the initial concentration of alloy component.

On the boundaries $\Gamma_{1i}(i = 1, 2)$ the following homogeneous boundary conditions of the second kind are given

$$\frac{\partial T_i}{\partial x}(x, t) = 0, \qquad (3)$$

whereas on the boundaries $\Gamma_{2i}(i = 1, 2)$ the boundary conditions of the third kind are given

$$-\lambda_i \frac{\partial T_i}{\partial x}(x, t) = \alpha(t)(T_i(x, t) - T_\infty), \qquad (4)$$

where $\alpha(t)$ is the heat-transfer coefficient and T_∞ is the ambient temperature.

On the phase change boundary Γ_g the temperature continuity condition and the Stefan condition are given

$$T_1(\xi(t), t) = T_2(\xi(t), t) = T^*(Z_L(t)), \qquad (5)$$

$$L\varrho_2 \frac{d\xi(t)}{dt} = -\lambda_1 \frac{\partial T_1(x, t)}{\partial x}\bigg|_{x=\xi(t)} + \lambda_2 \frac{\partial T_2(x, t)}{\partial x}\bigg|_{x=\xi(t)}, \qquad (6)$$

where T^* is the temperature of solidification, $Z_L(t)$ is the concentration of the alloy component on the phase change boundary at the liquid side, L is the latent heat of fusion, $\xi(t)$ is a function describing the location of the phase change boundary.

The process of macrosegregation, occurring in the alloy, is described by the Scheil model [14]. In this model, because of the diffusion coefficient in the solid phase is considerably smaller than in the liquid phase, it is assumed that $D_2 = 0$. On the other hand, the convection occurring in the liquid chase causes the leveling of the concentration of the alloy component in this phase, therefore it is assumed that $D_1 \rightarrow \infty$. Let us introduce the discretization of the interasol $[0, t^*]$ with nodes $t_i, i = 0, 1, ..., p^*$ and assume that the values of the concentrations at moments t_i, for $i = 1, 2, ..., p$, are known. Then, on the base of the mass balance of the alloy component in the cast domain for time t_{p+1}, the following equation may be derived

$$m_0 Z_0 = m_L(t_{p+1})Z_L(t_{p+1}) + \sum_{i=1}^{p+1} m_S(t_i)Z_S(t_i), \qquad (7)$$

where m_0 is the alloy mass, Z_0 is the initial concentration of the alloy component, $Z_L(t_i)$ and $Z_S(t_i)$ are concentrations of the alloy component on the phase change boundary in the liquid and solid phases at moment $t_i, m_L(t_i)$ and

$m_S(t_i)$ denote the alloy masses in the solid and liquid phases at moment t_i. Taking advantage of the partition coefficient $k = \frac{Z_S(t)}{Z_L(t)}$, the above equation may be transformed into the following form

$$Z_L\left(t_{p+1}\right) = \frac{m_0 Z_0 - \sum\limits_{i=1}^{p} m_S(t_i) Z_S(t_i)}{km_S\left(t_{p+1}\right) + m_L\left(t_{p+1}\right)}. \tag{8}$$

The examined domain is divided into control volumes V_j with the length of Δx_j, $j = 0, ..., n$. If the contribution of the solid phase in volume V_j at moment t is designated as $f_j(t)$, then the alloy mass at the solid and liquid states, contained in volume V_j at moment t, is expressed by the equation

$$m_{S,j}(t) = V_j \varrho_2 f_j(t), \tag{9}$$

$$m_{L,j}(t) = V_j \varrho_1 (1 - f_j(t)). \tag{10}$$

Making use of the above dependencies, equation (8) may be expressed as

$$Z_L\left(t_{p+1}\right) =$$
$$= \frac{b\varrho_1 Z_0 - \varrho_2 \sum\limits_{i=1}^{p} Z_S(t_i)\left(\sum\limits_{j=0}^{n}\left(\Delta x_j\left(f_j(t_i) - f_j(t_{i-1})\right)\right)\right)}{k\varrho_2 \sum\limits_{j=0}^{n}\left(\Delta x_j\left(f_j\left(t_{p+1}\right) - f_j\left(t_p\right)\right)\right) + \varrho_1 \sum\limits_{j=0}^{n}\left(\Delta x_j\left(1 - f_j\left(t_{p+1}\right)\right)\right)}. \tag{11}$$

In the discussed inverse problem for given temperature values ($(x_i, t_j) \in \Omega \times (0, t^*)$):

$$T(x_i, t_j) = U_{ij}, \quad i = 1, 2, ..., N_1, \quad j = 1, 2, ..., N_2, \tag{12}$$

where N_1 denotes the number of sensors, and N_2 the number of measurements taken from each sensor, the task is to designate the heat-transfer coefficient $\alpha(t)$. For known values of the heat-transfer coefficient the discussed problem becomes a direct problem, the solution of which will make it possible to derive temperatures $T_{ij} = T(x_i, t_j)$. Using the calculated temperatures T_{ij} and given temperatures U_{ij}, a functional determining the error of the approximate solution may be constructed

$$J(\alpha) = \sum_{i=1}^{N_1} \sum_{j=1}^{N_2} \left(T_{ij} - U_{ij}\right)^2. \tag{13}$$

3. Solution method

To solve a direct Stefan problem (equations (1)–(6)), the alternating phase truncation method was applied [11, 23]. In this method, in place of temperature T we insert an enthalpy

$$H(T) = \int_0^T c(u)\varrho(u)\,du + \eta(T)L\varrho_2, \tag{14}$$

where

$$\eta(T) = \begin{cases} 1 & \text{for } T > T^*\left(Z_L(t)\right), \\ 0 & \text{for } T \leqslant T^*\left(Z_L(t)\right). \end{cases} \tag{15}$$

Function $H(T)$ is discontinuous in the point given by the temperature of the phase change T^*. Its left-hand and right-hand limits at this point will be denoted as H_s and H_l:

$$H_s = \int_0^{T^*(Z_L(t))} c(u)\varrho(u)\,du, \tag{16}$$

$$H_l = H_s + L\varrho_2. \tag{17}$$

If we use equation (14) in the Stefan problem, we will obtain in both phases a heat conduction equation, where the temperature will be replaced with enthalpy.

The algorithm of the alternating phase truncation method (for one time's step) consists of two stages. In the first stage, we reduce the entire domain to a liquid phase, i.e. to the points at which the value of the enthalpy is smaller than H_l, we supply (conventionally) such quantity of heat, that the enthalpy equals to H_l. The, so obtained, heat transfer problem in a one-phase domain can be solved by one of the known methods (in the calculations we use the finite element method), obtaining thereby an approximate distribution of enthalpy. At points to which we have supplied a certain amount of heat, the same amount must be now deducted. After this operation we obtain the distribution of enthalpy, which is treated as a starting point for the second stage of calculations.

In the second stage, we reduce the whole domain to a solid phase, i.e. at those points of the domain, where the enthalpy value is higher than H_s, we carry away (symbolically) such amount of heat, that would allow the enthalpy to adopt a value equal H_s. Like in the first stage, we find an approximate distribution of enthalpy. At the end of the second stage, at the points where we artificially carried away a certain amount of heat, we add the same amount of heat. This completes the second stage and, at the same time, one step of the calculations (transfer from time t_i to time t_{i+1}) of the alternating phase truncation method.

The contribution of the solid phase in volume V_j at moment t is designated from the following relation

$$f_j(t) = \frac{H\left(x_j, t\right) - H_s}{H_l - H_s}, \tag{18}$$

where $H(x_j, t)$ denotes enthalpy at point $x_j \in V_j$ and at moment t (it is assumed, that the enthalpy is constant in the control volumes).

Next, on the base of (11), the value of the alloy concentration component $Z_L(t_{p+1})$ at moment t_{p+1} is calculated, designating, in this way, a new value of temperature solidification $T^*(Z_L(t_{p+1}))$, and, simultaneously, new boundary values of enthalpy H_s and H_l.

To find the minimum of the functional (13) a genetic algorithm is used. The calculations involve the use of real number representations of the chromosome and tournament selection. The algorithm also includes an elitist model, in which the best specimen of the previous population is remembered and, if in the current population all specimens are worse, the worst specimen of the current population is replaced by the remembered best specimen of the previous population. The study also uses arithmetical crossover operator and nonuniform mutation operator [23, 25]. The calculation were based on the following values of the genetic algorithm: population size $n_{pop} = 100$, number of generations $N = 100$, crossover probability $p_c = 0.7$ and mutation probability $p_m = 0.1$.

4. Example of computations

In the example the considered alloy was Cu-Zn (10% Zn) [14]: $b = 0.08$ [m], $\lambda_1 = \lambda_2 = 120$ [W/(m K)], $c_1 = c_2 = 390$ [J/(kg K)], $\varrho_1 = \varrho_2 = 8600$ [kg/m^3], $L = 190000$ [J/kg], $k = 0.855$, $Z_0 = 0.1$, temperature of solidification $T^*(Z_L) = 1356 - 473.68 Z_L$ [K], the ambient temperature $T_\infty = 298$ [K] and initial temperature $T_0 = 1323$ [K].

The values of four parameters: $\alpha_i, i = 1,2,3,4$, were designated in the inverse problem (Fig. 2):

$$\alpha(t) = \begin{cases} \frac{\alpha_2 - \alpha_1}{t_1} t + \alpha_1 & \text{for } t \in [0, t_1], \\ \frac{\alpha_3 - \alpha_2}{t_2 - t_1} t + \frac{\alpha_2 t_2 - \alpha_3 t_1}{t_2 - t_1} & \text{for } t \in (t_1, t_2], \\ \alpha_3 \exp\left(\frac{1}{t_3 - t_2} \ln\left(\frac{\alpha_4}{\alpha_3}\right)(t - t_2)\right) & \text{for } t \in (t_2, t^*], \\ \alpha_3 \exp\left(\frac{1}{t_3 - t_2} \ln\left(\frac{\alpha_4}{\alpha_3}\right)(t^* - t_2)\right) & \text{for } t > t^*, \end{cases}$$
$$(19)$$

where $t_1 = 38$, $t_2 = 93$, $t_3 = 350$, $t^* = 750$ [s]. The exact values of the heat transfer coefficient were as follows

$$\alpha_1 = 1200, \quad \alpha_2 = 800, \quad \alpha_3 = 600, \quad \alpha_4 = 250 [\text{W}/(\text{m}^2\text{K})].$$

It was assumed, that in the tested domain there is one thermocouple ($N_1 = 1$) placed at the distance of 10 mm from the domain boundary. Temperature readings were taken at every 0.1, 0.4, 1 and 4 s. The calculations were based on the exact values of temperature and on the values disturbed by random error with normal distribution and values 1%, 2% as well as 5%.

In Table 1, the results of reconstructing the sought parameters are compiled. The table contains the results derived for the exact input data and a variable number of the measurement points. It also specifies

the mean values of the designated parameters α_i (selected from 15 start-ups of the algorithm for different initial set-ups of the generator of the pseudo-random numbers), the relative percentage errors of the reconstruction of the parameters, and the values of standard deviations. It is clear, that at each time the boundary conditions are reconstructed with minimal errors, which are a consequence of the assumed criterion of ending the algorithm. In the case of the exact input data, the maximal error of the reconstruction of the sought parameters did not exceed 0.09%. The successive start-ups of the algorithm rendered similar results, which is proved by a low value of the standard deviation.
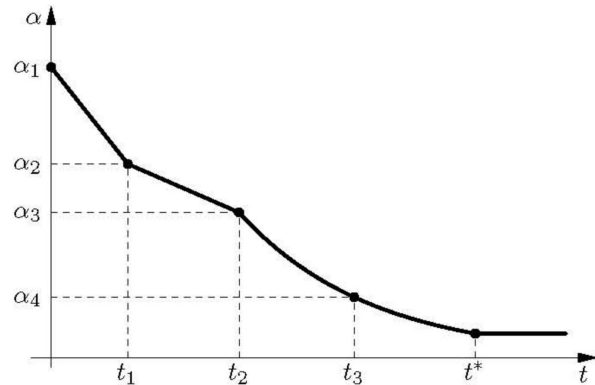

Fig. 2. Function $\alpha(t)$

Results of reconstructing the sought parameters for different number of the measurement points and exact input data (δ – value of the relative error, σ – value of the standard deviation)

α_i	δ[%]	σ	α_i	δ[%]	σ
0.1 s			0.4 s		
1200.051	0.0042	3.4419	1200.184	0.0154	2.8280
799.569	0.0539	3.0172	800.003	0.0003	2.2004
599.752	0.0413	1.1978	599.670	0.0550	0.8294
250.225	0.0899	0.2798	250.116	0.0462	0.2069
1 s			4 s		
1199.526	0.0395	1.0013	1200.503	0.0419	2.0637
800.041	0.0052	0.4542	799.918	0.0103	1.1462
600.095	0.0158	0.0887	599.934	0.0111	0.4178
249.972	0.0114	0.0383	250.023	0.0093	0.1774

In Figures 3 and 4, the reconstruction errors of the sought parameters are shown, for the case in which the initial data were burdened with disturbance. Figure 3 illustrates the results obtained in the case of temperature readings taken at every 0.1 s and 4 s for different values of the disturbances in the input data. Figure 4 shows the results obtained for the input data burdened by the
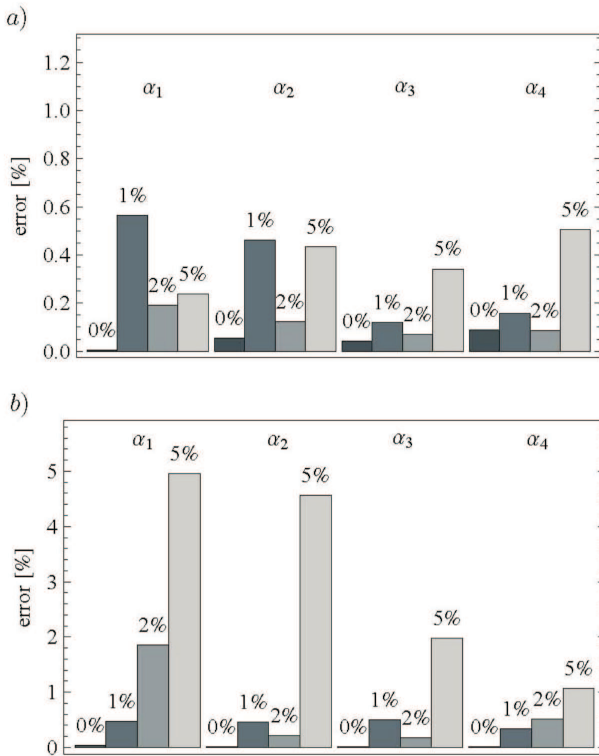
Fig. 3. Errors in the reconstruction of the heat transfer coefficient for temperature measurements at every 0.1s (a) and 4s (b) and different errors in the input
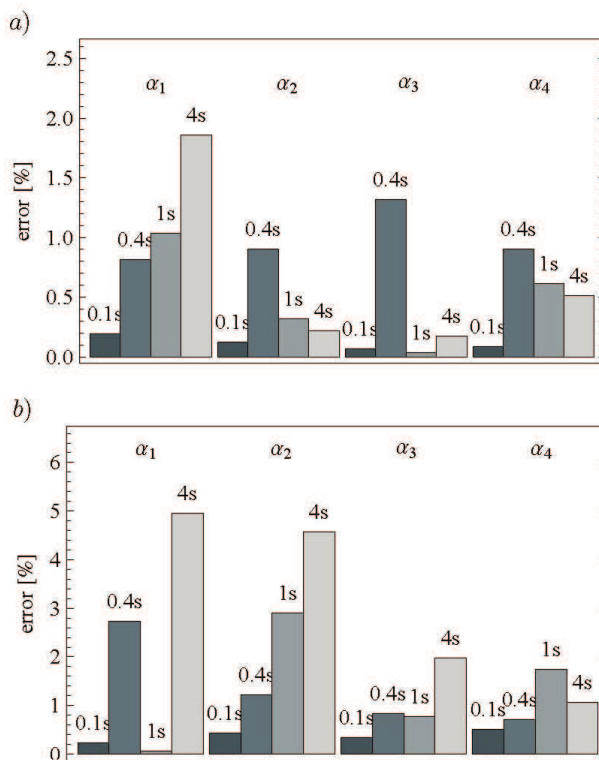

Fig. 4. Errors in the reconstruction of the heat transfer coefficient for different number of temperature measurements (calculations for data burdened by errors of 2% (a) and 5% (b))

disturbance of 2% and 5% and for different number of the control points (temperature measurements taken at every 0.1, 0.4, 1 and 4s). It may be observed, that in each case the errors in the reconstruction of the boundary conditions (with disturbed initial data) are smaller than the initial data errors. In the case of the disturbance of 1% the errors did not exceed 0.62%, for the disturbance of 2% the errors did not exceed 1.86%; whereas, for the disturbance of 5% the errors did not exceed 4.96%. The increase in the number of the control points or the decrease in the value of the initial data cause more exact reconstruction of the values of the sought parameters.

In Table 2, the errors of the reconstruction of temperature at the measuring point are compiled at each 1 s and 4 s. Whereas, in Figure 5, the absolute errors of the reconstruction of temperature at the measuring point are compiled for the exact input data and for the data burdened by errors 5% and the temperature measurement at each 4 s. As seen from the results, the temperature distribution is reconstructed very well every single time. The biggest discrepancy occurred for the smallest number of the measurement points and the biggest disturbance of the initial data. In such case, the absolute reconstruction error was 7.5741 K, whereas the mean value of the absolute error was equal to 1.7618 K. The relative errors were 0.5826% and 0.1483%, respectively. For more measurements or minor input data errors the differences in the reconstruction of the temperature distribution were smaller. For example, for temperature readings taken at every 0.1 s and the exact input data the errors were: 0.0641 K, 0.0354 K, 0.0053% and 0.003 %.

TABLE 2

Errors in the reconstruction of temperature at the measurement point for temperature measurements taken at every 1 s and 4 s (Δ_{mean} – mean value of the absolute error, Δ_{max} – maximum value of the absolute error, δ_{mean} – mean value of the relative error, δ_{max} – maximum value of the relative error)

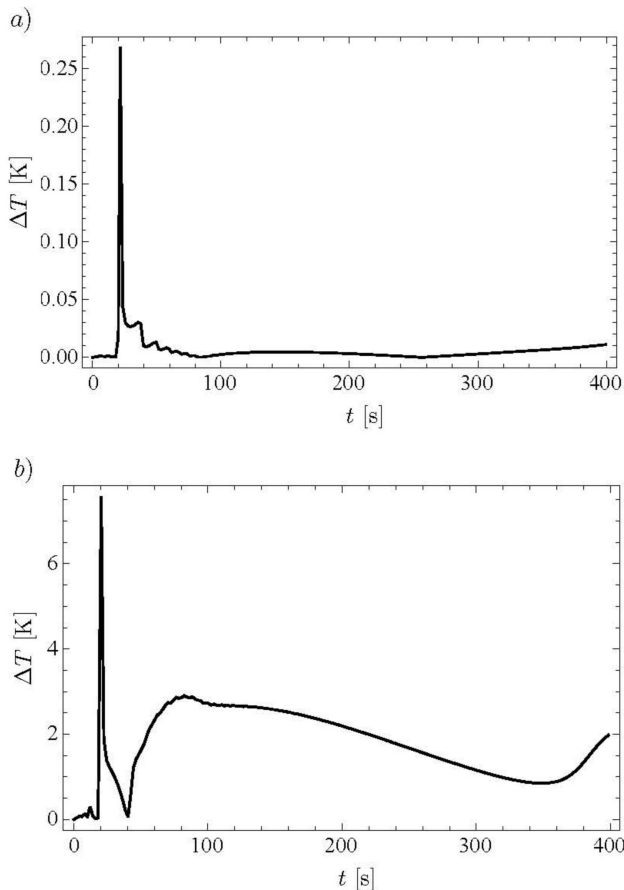| Per	0%	1%	2%	5%
1s				
Δ_{mean} [K]	0.0063	0.1770	0.3054	1.3676
Δ_{max} [K]	0.2786	5.0424	6.8117	6.1970
δ_{mean} [%]	0.0005	0.0150	0.0254	0.1155
δ_{max} [%]	0.0215	0.3856	0.5237	0.4739
4s				
Δ_{mean} [K]	0.0050	0.1935	0.6595	1.7618
Δ_{max} [K]	0.2687	5.1121	7.2629	7.5741
δ_{mean} [%]	0.0004	0.0163	0.0554	0.1483
δ_{max} [%]	0.0207	0.3910	0.5554	0.5826

284

a)

b)

Fig. 5. The absolute errors of the reconstruction of the temperature at the measurement point for temperature measurements taken at every 4 s (calculations for the exact input data (a) and the input data burdened by errors of 5% (b))

5. Conclusions

The presented examples of calculations show a very good approximation of the exact solution and stability of the algorithm in terms of the input data errors. According to the results, any increase in the control points or decrease in the input data errors result in more exact reconstruction of the values of the parameters, and, at the same time, better reconstruction of the exact temperature distribution.

REFERENCES

[1] V. A l e x i a d e s, A. D. S o l o m o n, Mathematical Modeling of Melting and Freezing Processes, Hemisphere Publ. Corp., Washington 1993.

[2] J. C r a n k, Free and Moving Boundary Problems, Clarendon Press, Oxford 1996.

[3] B. G a n a p a t h y s u b r a m a n i a n, N. Z a b a r a s, Control of solidification of nonconducting materials using tailored magnetic fields, J. Crystal Growth **276**, 299-316 (2005).

[4] B. G a n a p a t h y s u b r a m a n i a n, N. Z a b a r a s, On the control of solidification using magnetic fields and magnetic field gradients, Int. J. Heat Mass Transfer **48**, 4174-4189 (2005).

[5] R. G r z y m k o w s k i, D. S ł o t a, Numerical method for multi-phase inverse Stefan design problems, Arch. Metall. Mater. **51**, 161-172 (2006).

[6] R. G r z y m k o w s k i, D. S ł o t a, One-phase inverse Stefan problems solved by Adomian decomposition method, Comput. Math. Appl. **51**, 33-40 (2006).

[7] S. C. G u p t a, The Classical Stefan Problem. Basic Concepts, Modelling and Analysis, Elsevier, Amsterdam 2003.

[8] M. H o j n y, M. G ł o w a c k i, The methodology of strain-stress curves determination for steel in semi-solid state, Arch. Metall. Mater. **54**, 475-483 (2009).

[9] A. I m a n i, A. A. R a n j b a r, M. E s m k h a n i, Simultaneous estimation of temperature-dependent thermal conductivity and heat capacity based on modified genetic algorithm, Inverse Probl. Sci. Eng. **14**, 767-783 (2006).

[10] W. K a p t u r k i e w i c z, E. F r a ś, A. A. B u r b e l k o, Modeling the kinetics of solidification of cast iron with lamellar graphite, Arch. Metall. Mater. **54**, 369-380 (2009).

[11] E. M a j c h r z a k, B. M o c h n a c k i, Application of the BEM in the thermal theory of foundry, Eng. Anal. Bound. Elem. **16**, 99-121 (1995).

[12] E. M a j c h r z a k, R. S z o p a, Simulation ofheat and mass transferindomain of solidifying binary alloy, Arch. Metallurgy **43**, 341-351 (1998).

[13] G. H. M e y e r, A numerical method for the solidification of a binary alloy, Int. J. Heat Mass Transfer **24**, 778-781 (1981).

[14] B. M o c h n a c k i, E. M a j c h r z a k, R. S z o p a, Simulation of heat and mass transfer in domain of casting made from binary alloy, Arch. Foundry Eng. **8 (4)**, 121-126 (2008).

[15] B. M o c h n a c k i, J. S. S u c h y, Numerical Methods in Computations of Foundry Processes, PFTA, Cracow 1995.

[16] B. M o c h n a c k i, J. S. S u c h y, M. P r a ż m o w s k i, Modelling of segregation in the process of Al-Si alloy solidification, Soldification of Metals and Alloys **2 (44)**, 229-234 (2000).

[17] K. O k a m o t o, B. Q. L i, A regularization method for the inverse design of solidification processes with natural convection, Int. J. Heat Mass Transfer **50**, 4409-4423 (2007).

[18] M. N. Ö z i ş i k, Heat Conduction, Wiley & Sons, New York 1980.

[19] H.-S. R e n, Application of the heat-balance integral to an inverse Stefan problem, Int. J. Therm. Sci. **46**, 118-127 (2007).

[20] D. S a m a n t a, N. Z a b a r a s, Numerical study of macrosegregation in aluminum alloys solidifying on uneven surfaces, Int. J. Heat Mass Transfer **48**, 4541-4556 (2005).

[21] D. S a m a n t a, N. Z a b a r a s, Control of macrosegregation during the solidification of alloys using magnetic fields, Int. J. Heat Mass Transfer **49**, 4850-4866 (2006).

[22] D. S ł o t a, Direct and inverse one-phase Stefan problem solved by variational iteration method, Comput. Math. Appl. **54**, 1139-1146 (2007).

[23] D. S ł o t a, Solving the inverse Stefan design problem using genetic algorithms, Inverse Probl. Sci. Eng. **16**, 829-846 (2008).

[24] D. S ł o t a, Using genetic algorithms for the determination of an heat transfer coefficient in three-phase inverse Stefan problem, Int. Comm. Heat & Mass Transf. **35**, 149-156 (2008).

[25] D. S ł o t a, Identification of the cooling condition in 2-D and 3-D continuous casting processes, Numer. Heat Transfer B **55**, 155-176 (2009).

[26] D. S ł o t a, The application of the homotopy perturbation method to one-phase inverse Stefan problem, Int. Comm. Heat & Mass Transf. **37**, 587-592 (2010).

[27] J. S. S u c h y, B. M o c h n a c k i, Analysis of segregation process using the broken line model. Theoretical base, Arch. Foundry **3 (10)**, 229-234 (2003).

[28] D. S z e l i g a, J. G a w ę d a, M. P i e t r z y k, Parameters identification of material models based on the inverse analysis, Int. J. Appl. Math. Comput. Sci. **14**, 549-556 (2004).

[29] R. S z o p a, Modelling of solidification and crystalization using combined boundary element method, Zeszyty Nauk. Pol. Śl. Hut. **54** (1999).

[30] J. T a l a r, D. S z e l i g a, M. P i e t r z y k, Application of genetic algorithm for identification of rheological and friction parameters in copper deformation process, Arch. Metallurgy **47**, 27-41 (2002).

[31] V. R. V o l l e r, A similarity solution for solidification of an under-cooled binary alloy, Int. J. Heat Mass Transfer **49**, 1981-1985 (2006).

[32] V. R. V o l l e r, An enthalpy method for modeling dendritic growth in a binary alloy, Int. J. Heat Mass Transfer **51**, 823-834 (2008).

[33] G. Z. Y a n g, N. Z a b a r a s, The adjoint method for an inverse design problem in the directional solidification of binary alloys, J. Comput. Phys. **140**, 432-452 (1998).

[34] G. Z. Y a n g, N. Z a b a r a s, An adjoint method for the inverse design of solidification processes with natural convection, Int. J. Numer. Methods Engrg. **42**, 1121-1144 (1998).

[35] N. Z a b a r a s, G. Z. Y a n g, A functional optimization formulation and implementation of the inverse natural convection problem, Comput. Methods Appl. Mech. Engrg. **144**, 245-274 (1997).